 https://doi.org/10.1051/e3sconf/202337601084

Calculation model for lubrication of bearings with unconventional support surface profile and fusible shaft surface coating

G. Badakhov[1], *N.* Zinoviev[1], *M.* Mukutadze[1*], and *V.* Shvedova[1]

[1]Rostov State Transport University, 2, Rostovskogo Strelkovogo Polka Narodnogo Opolcheniya sq., 344038, Rostov-on-Don, Russia

Abstract. This research work uses the true viscous fluid flow equation for the thin layer, the continuity equation, and the equation describing the radius of the fused shaft coated with a metal alloy taking into account the mechanical energy dissipation rate formula to find the asymptotic and the exact self-similar solution for the zero and first-order approximation for the radial sliding bearing with the support profile adapted to friction and light-alloy coating for incomplete filling of the working gap. We obtained the analytical dependencies for the fused surface radius of metal coating and the speed and pressure field. Besides, we determined the key operating parameters of the reviewed friction couple, the carrying capacity, and the friction force. The authors assess the impact of the parameters associated with the fusing of the coating of the friction-adapted support profile and the length of the loaded area on the carrying capacity and the friction force.

1 Introduction

A large number of research works focus on the development of a calculation model for radial sliding bearings with metal coating [1-12]. However, lubrication on fused coatings is not a self-sustaining process. To ensure self-sustaining lubrication of sliding bearings, it is necessary that one of the contact surfaces had metal coating and there was always some lubricant present, which can be achieved by the continuous feeding of the lubricant or by using a porous coating on the other contact surface [13-26], or by using an unconventional support profile.

In this work, we present a calculation model for the radial sliding bearing with an unconventional bushing support profile and metal-coated shaft for the incomplete filling for the working gap to ensure salt-sustaining hydrodynamic flow.

2 Statement of Problem

We review the stable flow of true viscous fluid between the eccentric shaft and bearing. The bearing with non-circular support is fixed, and the shaft with a metal surface coating is

[*] Corresponding author: Murman1963@yandex.ru

rotating at an angular speed Ω. In the polar coordinate system (Figure 1) r', θ with the pole in the center of the shaft, the equations of metal coating shaft C_1, fused surface shaft C_0, adapted support profile bushing C_2, and the bearing bushing can be written down as follows:

$$C_1 : r' = r_0, \quad C_0 : r' = r_0 - \lambda' f(\theta), \; C_2 : r' = r_1(1+H) - a' \sin \omega \theta = h'(\theta), \quad C_3 : r' = r_1(1+H), \tag{1}$$

Where $H = \varepsilon \cos \theta - \frac{1}{2}\varepsilon^2 \sin^2 \theta + \ldots, \quad \varepsilon = \frac{e}{r_0}$,

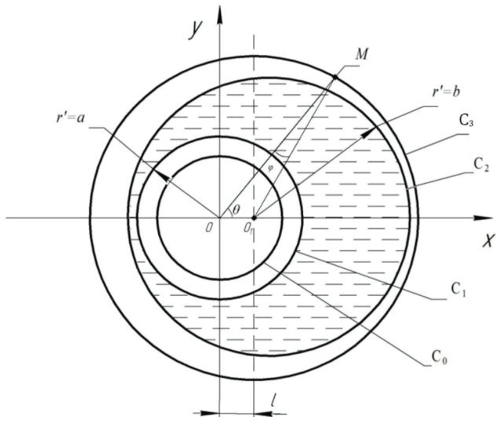

Fig. 1. Calculation model.

The basic equations include the flow equation for the true incompressible viscous fluid, the continuity equation, and the equation describing the radius of the fused shaft coated taking into account the mechanical energy dissipation rate:

$$\frac{\partial p'}{\partial r'} = 0; \qquad \mu \frac{\partial^2 v_\theta}{\partial r'^2} = \frac{dp'}{d\theta}; \frac{\partial v_{r'}}{\partial r'} + \frac{v_{r'}}{r'} + \frac{1}{r'}\frac{\partial v_\theta}{\partial \theta} = 0;$$

$$-\frac{d\lambda' f(\theta) r_0}{d\theta} \Omega L' = 2\mu \int_{r_0 - \lambda' f(\theta)}^{h'(\theta)} \left(\frac{\partial v_\theta}{\partial r'}\right)^2 dr', \tag{2}$$

Equation system (2) is solved under the following boundary conditions:

$$v_\theta = 0, v_{r'} = 0 \text{ at } r' = r_1(1+H) - a' \sin \omega \theta;$$

$$v_{r'} = 0, v_\theta = \Omega\left(r_0 - \lambda' f(\theta)\right) \text{ at } r' = r_0 - \lambda' f(\theta);$$

$$p'(\theta_1) = p'(\theta_2) = 0; \quad r_0 - \lambda' f(\theta) = h_0^* \text{ at } \theta = \theta_1, \quad \theta = \theta_2 \tag{3}$$

The transition to non-dimensional variables is done using the following formulae:

$$r' = \left(r_0 - \lambda' f(\theta)\right) + \delta r; \quad \delta = r_1 - \left(r_0 - \lambda' f(\theta)\right); \quad v_{r'} = \Omega \delta u, \quad v_\theta = \Omega v \left(r_0 - \lambda' f(\theta)\right);$$

$$p' = p^* p; \quad p^* = \frac{\mu \Omega \left(r_0 - \lambda' f(\theta)\right)^2}{\delta^2}. \tag{4}$$

If we insert (4) in the system of differential equations (2) and (3), we get:

$$\frac{\partial p}{\partial r}=0; \qquad \frac{\partial^2 v}{\partial r^2}=\frac{dp}{d\theta};\frac{\partial u}{\partial r}+\frac{\partial v}{\partial \theta}=0;$$

$$\frac{d\Phi(\theta)}{d\theta}=-K\int_{-\Phi(\theta)}^{h(\theta)}\left(\frac{\partial v}{\partial r}\right)^2 dr, \tag{5}$$

Where $K=\frac{2\mu\Omega\left(r_0-\lambda' f(\theta)\right)}{L'\delta}$; $\quad \eta=\frac{e}{\delta}$; $\quad \eta_1=\frac{a'}{\delta}$; $\Phi(\theta)=\lambda' f(\theta)$.

$$u=0, \quad v=1 \text{at } r=r_0-\Phi(\theta);$$

$$u=0, v=0 \text{at } r=1+\eta\cos\theta-\eta_1\sin\omega\theta=h(\theta);$$

$$p'(\theta_1)=p'(\theta_2)=0; \tag{6}$$

If we assume that K is a small parameter determined by the fusing, we can express the asymptotic solution as a system of differential equations (5)-(6), and find

$$v(r,\theta)=v_0(r,\theta)+Kv_1(r,\theta)+K^2v_2(r,\theta)+\dots;$$

$$u(r,\theta)=u_0(r,\theta)+Ku_1(r,\theta)+K^2u_2(r,\theta)+\dots; \tag{7}$$

$$\Phi(\theta)=-K\Phi_1(\theta)-K^2\Phi_2(\theta)-K^3\Phi_3(\theta)-\dots;$$

$$p(\theta)=p_0(\theta)+Kp_1(\theta)+K^2p_2(\theta)+K^3p_3(\theta)\dots$$

If we insert (7) in the system of (5)-(6):
– for the zero approximation:

$$\frac{\partial^2 v_0}{\partial r^2}=\frac{dp_0}{d\theta},\frac{\partial v_0}{\partial \theta}+\frac{\partial u_0}{\partial r}=0; \tag{8}$$

$$v_0=0, u_0=0 \text{ at } r=1+\eta\cos\theta-\eta_1\sin\omega\theta;$$

$$v_0=1, u_0=0 \text{ at } r=r_0-\Phi(\theta); \quad p_0(\theta_1)=p_0(\theta_2)=0; \tag{9}$$

– for the first approximation:

$$\frac{\partial^2 v_1}{\partial r^2}=\frac{dp_1}{d\theta}; \quad \frac{\partial v_1}{\partial \theta}+\frac{\partial u_1}{\partial r}=0; \ \frac{d\Phi_1(\theta)}{d\theta}=-K\int_0^{h(\theta)}\left(\frac{\partial v_0}{\partial r}\right)^2 dr; \tag{10}$$

$$v_1=\left(\frac{\partial v_0}{\partial r}\right)_{r=0}\cdot\widetilde{\Phi}; u_1=\left(\frac{\partial u_0}{\partial r}\right)\Big|_{r=0}\cdot\widetilde{\Phi};$$

$$v_1=0u_1=0 \text{ at } r=h(\theta)+\widetilde{\Phi};$$

$$p_1(\theta_1)=p_1(\theta_2)=0; \tag{11}$$

The self-similar solution for the zero approximation can be found as follows:

$$v_0 = \frac{\partial\psi_0}{\partial r} + V_0(r,\theta); \quad u_0 = -\frac{\partial\psi_0}{\partial\theta} + U_0(r,\theta); \ \psi_0(r,\theta) = \tilde{\psi}_0(\xi); \quad \xi = \frac{r}{h(\theta)};$$

$$V_0(r,\theta) = \tilde{v}(\xi); \quad U_0(r,\theta) = -\tilde{u}_0(\xi)\cdot h'(\theta). \tag{12}$$

If we insert (12) in (10)-(11), we get the following analytical expressions:

$$\tilde{\psi}_0'(\xi) = \frac{\tilde{C}_2}{2}(\xi^2-\xi), \tilde{v}_0(\xi) = \tilde{C}_1\frac{\xi^2}{2} - \left(1+\frac{\tilde{C}_1}{2}\right)\xi + 1, \quad \tilde{C}_1 = 6.$$

$$\tilde{C}_2 = -6\left(1 + \frac{\eta}{\theta_2-\theta_1}(\sin\theta_2 - \sin\theta_1) + \frac{\eta_1}{\omega(\theta_2-\theta_1)}(\cos\omega\,\theta_2 - \cos\omega\,\theta_1)\right).$$

$$p_0 = 6\left(\eta(\sin\theta - \sin\theta_1) + \frac{\eta_1}{\omega}(\cos\omega\,\theta - \cos\omega\,\theta_1) - \right.$$
$$\left. -\frac{\eta(\theta-\theta_1)}{\theta_2-\theta_1}(\sin\theta - \sin\theta_1) - \frac{\eta_1(\theta-\theta_1)}{\omega(\theta_2-\theta_1)}(\cos\omega\,\theta_2 - \cos\omega\,\theta_1)\right) \tag{13}$$

To determine $\Phi_1(\theta)$, we use (13):

$$\Phi_1(\theta) = \theta - \eta\sin\theta - \frac{\eta_1}{\omega}\cos\omega\,\theta + h_0^*; \tag{14}$$

$$\tilde{\psi}_1'(\xi) = \frac{\tilde{\tilde{C}}_2}{2}(\xi^2-\xi), \tilde{v}_1(\xi) = \tilde{\tilde{C}}_1\frac{\xi^2}{2} + \left(\frac{\tilde{\tilde{C}}_1}{2} - M\right)\xi + M, \quad \tilde{\tilde{C}}_1 = 6M.$$
$$\tilde{\tilde{C}}_2 = -6M(1+\tilde{\Phi})\left(1 + \frac{\tilde{\eta}}{\theta_2-\theta_1}(\sin\theta_2 - \sin\theta_1) + \frac{\tilde{\eta}_1}{\omega(\theta_2-\theta_1)}(\cos\omega\,\theta_2 - \cos\omega\,\theta_1)\right) \tag{15}$$

$$p_1 = \frac{6M}{(1+\tilde{\Phi})^2}\left[\eta(\sin\theta_2 - \sin\theta) + \frac{\eta_1}{\omega}(\cos\theta_2 - \cos\theta) - \right.$$
$$\left. -\frac{\tilde{\eta}(\theta_2-\theta)}{\theta_2-\theta_1}(\sin\theta_2 - \sin\theta_1) - \frac{\tilde{\eta}_1(\theta_2-\theta)}{\omega(\theta_2-\theta_1)}(\cos\theta_2 - \cos\theta_1)\right]$$

where $\tilde{\eta} = \frac{\eta}{1+\tilde{\Phi}}, \quad \tilde{\eta}_1 = \frac{\eta_1}{1+\tilde{\Phi}};$

$$M = \sup_{\theta\in[\theta_1;\theta_2]} \left.\frac{\partial v_0}{\partial r}\right|_{r=0} \cdot \tilde{\Phi} = \sup_{\theta\in[\theta_1;\theta_2]} |(-1 - 4\eta\cos\theta + 4\eta_1\sin\omega\,\theta +$$
$$+\frac{3\eta}{\theta_2-\theta_1}(\sin\theta_2 - \sin\theta_1) + \frac{3\eta_1}{\omega(\theta_2-\theta_1)}(\cos\omega\,\theta_2 - \cos\omega\,\theta_1)| \cdot \tilde{\Phi}.$$

$$p_1 = \frac{6M}{(1+\tilde{\Phi})^2}\left[\eta(\sin\theta_2 - \sin\theta) + \frac{\eta_1}{\omega}(\cos\theta_2 - \cos\theta) - \right.$$
$$\left. -\frac{\tilde{\eta}(\theta_2-\theta)}{\theta_2-\theta_1}(\sin\theta_2 - \sin\theta_1) - \frac{\tilde{\eta}_1(\theta_2-\theta)}{\omega(\theta_2-\theta_1)}(\cos\theta_2 - \cos\theta_1)\right]$$

Considering (8), (10), (13), and (15) for the carrying capacity and the friction force

$$R_x = p^* r_0 \int_{\theta_1}^{\theta_2} (p_0 + K p_1) \cos\theta \, d\theta;$$

$$\mathrm{R_y} = \mathrm{p^* r_0} \int_{\theta_1}^{\theta_2} (\mathrm{p_0} + \mathrm{K p_1}) \sin\theta \, d\theta;$$

$$\mathrm{L_{fr}} = \mu \int_{\theta_1}^{\theta_2} \left[\left.\frac{\partial v_0}{\partial r}\right|_{r=0} + K \left.\frac{\partial v_1}{\partial r}\right|_{r=0} \right] d\theta. \tag{16}$$

Theoretical research showed that for the rheologic properties of the lubricant and the metal coating fuse with true viscous properties, the metal coating and adapted profile make the carrying capacity increase ≈ by10-12% along with the growth of the parameter characterizing the rheologic properties of the lubricant, ω characterizing the adapted profile, and the length of loaded area $(\theta_2 - \theta_1)$ while the friction coefficient is reducing ≈ by 12-14%.

3 Experimentation

During the experiments, we analyzed the sliding support with Wood's ally coating and a profile adapted to friction loads. We determined the value of the friction coefficient that helps assess the hydrodynamic friction regime for the bearing with a Newtonian lubricant and the surface coating fuse. The analysis of experimental data shows that coating fuse and support profile have a greater impact on the friction coefficient than the rheologic properties of the lubricants used. The conducted experiments confirm the validity of the developed theoretical models and their numerical analysis data within the given range of design and operation parameters. The agreement of theoretical and experimental results is satisfactory.

Table 1. Results.

No.		**Theoretical result**		**Experimental result**
		coating	**adapted-profile coating**	**adapted-profile coating**
Friction coefficient	1	0.0034	0.0017	0.0019
	2	0.0036	0.0018	0.0020
	3	0.0039	0.0019	0.0022
	4	0.0038	0.0020	0.0025
	5	0.0041	0.0021	0.0024

4 Conclusion

The authors developed new multi-parameter expressions for the key operating parameters taking into account the rheologic properties of a true viscous lubricant and surface coat fuse for the incomplete filling of the running gap, taking into account the support profile adapted for friction.

The authors assessed the impact of variable factors associated with the surface fusing and friction-adapted support profile for the incomplete filling of the running gap.

The obtained adjusted calculation models allow for the use of various combinations of metal coating and friction-adapted support profile to adjust the proportion of the carrying capacity and the friction coefficient.

The agreement of the theoretical and experimental data is sufficient, and the theoretical assumptions are confirmed.

Symbols

r_0 – is the radius of the coated shaft; r_1 is the radius of the bushing; e is the eccentricity; ε is relative eccentricity; $\lambda' f(\theta)$ is the function determining the profile of the fused shaft coating; a' и ω are the disturbance range and the adapted bushing profile parameter respectively, v_θ, $v_{r'}$ and the components of the lubrication medium speed vector; p' is the hydrodynamic pressure; μ is the dynamic viscosity coefficient; $L^{'}$ is the specific fusing heat per a unit of volume.

References

1. M.E. Bondarenko, R.N. Polyakov, Li. Shengbo, Materials Science and Engineering **1001(1),** 012078 (2020) DOI: 10.1088/1757-899X/1001/1/012078
2. R.N. Polyakov, A.A. Revkov, Fu. Shengping, L.I. Shengbo, Materials Science and Engineering **1001(1)**, 012003 (2020) DOI: 10.1088/1757-899X/1001/1/012003
3. R.N. Polyakov, N.V. Krupenin, I.E. Kudryavcev, V.V. Romanov, I.N. Stebakov, Journal of Physics: Conference Series **1515**, 052063 (2020) DOI: 10.1088/1742-6596/1515/5/052063
4. Y. Kazakov, A. Kornaev, R. Polyakov, RusAutoCon **9208118**, (2020) 336–340
5. R. Polyakov, S. Majorov, I. Kudryavcev, N. Krupenin, Vibroengineering Procedia **30**, 61–67 (2020)
6. A.N. Opatskikh, S.A. Solop, I.A. Kolobov, Materials Science and Engineering, 012033 (2019)
7. A.N. Opatskikh, S.A. Solop, S.S. Chernyaev, Russian Engineering Research 39, 8 (2019)
8. K.S. Akhverdiev, et all., Journal of Machinery Manufacture and Reliability **4**, 359-365 (2011)
9. M.A. Mukutadze, E.O. Lagunova, V.V. Vasilenko, Journal of Machinery Manufacture and Reliability **47**, 271-277 (2018)
10. E. Zadorozhnaya, V. Hudyakov, I. Dolgushin, Lecture Notes in Mechanical Engineering, 1183-1193 (2020) DOI: 10.1007/978-3-030-22041-9_123
11. I.G. Levanov, E.A. Zadorozhnaya, I.V. Mukhortov, M.O. Eschiganov, Tribology in Industry **42(3)**, 461-467 (2020) DOI: 10.24874/ti.708.06.19.08
12. M. Kandeva, Y.V. Rozhdestvensky, P. Svoboda, Z. Kalitchin, E. Zadorozhnaya, Journal of Environmental Protection and Ecology **21(1)**, 222-233 (2020)
13. E. Zadorozhnaya, I. Levanov, M. Kandeva, Current state of research, Lecture Notes in Mechanical Engineering **0(9783319956299)**, 939-947 (2019) DOI: 10.1007/978-3-319-95630-5_98
14. I. Levanov, E. Zadorozhnaya, D. Vichnyakov, Lecture Notes in Mechanical Engineering **0(9783319956299)**, 967-972 (2019) DOI: 10.1007/978-3-319-95630-5_101
15. I. Mukhortov, E. Zadorozhnaya, M. Kandeva, I. Levanov, Tribology in Industry **41(3)**, 355-364 (2019) DOI: 10.24874/ti.2019.41.03.05

16. I. Levanov, E. Zadorozhnaya, M. Kandeva, Z. Kalitchin, N. Dolgushina, E. Polyacko, Journal of Environmental Protection and Ecology **20(3)**, 1303-1309 (2019)
17. E. Zadorozhnaya, S. Sibiryakov, V. Hudyakov, Tribology in Industry **39(4)**, 452-459 (2017) DOI: 10.24874/ti.2017.39.04.04
18. I.V. Mukchortov, K.A. Pochkaylo, E.A. Zadorozhnaya, Procedia Engineering **150**, 607-611 (2016) DOI: 10.1016/j.proeng.2016.07.052
19. K.S. Akhverdiev, A.M. Mukutadze, Mechanical Engineering Research **6(2)**, 1–10 (2016)
20. I.V. Kolesnikov, A.M. Mukutadze, V.V. Avilov, Ways of Increasing Wear Resistance and Damping Properties of Radial Bearings with Forced Lubricant supply, Proceedings of the 4th International Conference on Industrial Engineering, Lecture Notes in Mechanical Engineering, ICIE, pp. 1049 – 1062 (2018)
21. A.M. Mukutadze, Procedia Engineering **150**, 547–558 (2016)
22. K.S. Akhverdiev, N.S. Zadorozhnaya, A.M. Mukutadze, B.M. Flek, Journal of Machinery Manufacture and Reliability **45(3)**, 247–251 (2016)
23. E.O. Lagunova, M.A. Mukutadze, Journal of Friction and Wear **40(1)**, 88-94 (2019)
24. K.S. Akhverdiev, A.M. Mukutadze, N.S. Zadorozhnaya, B.M. Flek, Journal of Friction and Wear **37(4)**, 395–400 (2016)
25. K.S. Akhverdiev, A.M. Mukutadze, International Journal of Applied Engineering Research **1**, 76–85 (2017)
26. G.V. Darovskoy, V.N. Polyakov, A.N Opatskikh, Materials Science and Engineering **996(1)**, 012010 (2020)